Salt-Induced Structural Behavior for Poly(*N*-isopropylacryamide) Grafted onto Solid Surface Observed Directly by AFM and QCM-D

Naoyuki Ishida[†,‡] and Simon Biggs*[,†]

Institute of Particle Science & Engineering, School of Process, Environmental and Materials Engineering, University of Leeds, Leeds LS2 9JT, United Kingdom, and Research Institute of Environmental Management Technology, National Institute of Advanced Industrial Science and Technology (AIST), 16-1 Onogawa, Tsukuba 306-8569, Japan

Received August 20, 2007; Revised Manuscript Received September 16, 2007

ABSTRACT: The salt-induced structural changes of an end-grafted poly(*N*-isopropylacrylamide) (PNIPAM) layer on a silica substrate were investigated in sodium sulfate solutions using an atomic force microscope (AFM) and a quartz crystal microbalance with dissipation (QCM-D). A PNIPAM layer was grafted onto the silicon wafer surface by free radical polymerization of NIPAM to obtain a high molecular weight polymer layer with low grafting density overall. AFM images of the coated surface were featureless at low salt concentrations commensurate with a brush-like layer. At salt concentrations ≥0.11 M, a large number of domain structures, with a characteristic size of ∼100 nm, were seen on the surface commensurate with a collapse of the brush-like layer into mushroom-like aggregates. This critical concentration for brush collapse is in good agreement with the concentration range of between 0.1 and 0.2 M, at which the phase transition of the bulk PNIPAM is reported. Both the frequency and the dissipation data obtained using a QCM-D also showed a significant change at this concentration indicative of the layer collapse. Further analysis of these data confirmed that the observed PNIPAM structural transition was caused by a collapse of the brush-like structure as a result of dehydration of the polymer chains.

Introduction

Poly(*N*-isopropylacrylamide) (PNIPAM) has a lower critical solution temperature (LCST) of around 32 °C[1] and shows a sharp phase transition in aqueous solutions across the LCST. Below the LCST, PNIPAM chains have an expanded conformation in solution, while they shrink to take a globular form at temperatures higher than the LCST. Grafting of PNIPAM to solid surfaces is a promising method for creating various intelligent surfaces, as the surface properties may be readily controlled simply by changing the temperature due to this thermal response. Such surfaces have been explored for a variety of applications including liquid chromatography,[2,3] permeation-controlled filters,[4,5] chemical sensors,[6] attachment−detachment controllable surfaces for proteins[7] and living cells,[8−10] and functional composite surfaces.[11] A detailed understanding of the properties of such grafted polymer layers is therefore crucial if they are to be successfully employed in these proposed applications. As a result, the thermo-responsive properties of PNIPAM layers grafted onto solid surface have been extensively studied using techniques such as dynamic light scattering,[12,13] surface plasmon resonance,[14] neutron reflectivity,[15−18] quartz crystal microbalance,[19−21] and atomic force microscopy.[22,23]

The phase transition of PNIPAM is also effected by the presence of salts in the background solution; for example, the LCST of PNIPAM is dependent on the type and concentration of salt present. Similar effects are also seen with other non-ionic polymers such as methylcellulose[24] and poly(vinyl acetate).[25] Such salt-dependent effects for free PNIPAM in aqueous solution have been often related to the Hofmeister (lyotropic) series for anions. This series originally ranked the potential of the salts to precipitate proteins, and the empirical order is known to be SO_4^{2-} > Cl > Br > I > SCN.[26,27] It has since been shown over many years that salts can act both to enhance and to decrease the solubility of different polymers, effects that are known as "salting-in" and "salting-out", respectively. It has been generally assumed that the "salting-out" effect of anions such as sulfate is caused by a dehydration of the PNIPAM chains as a result of two main effects of the salt. In the first, it is thought that sulfate ions can interfere with the hydrogen bonding between amides in the polymer and water molecules. In addition, it is believed that the structure of the water shell around the isopropyl groups in side chains and hydrocarbons in the backbone of the polymer formed by hydrophobic hydration may be also destabilized by the salts.

Although the effects of salts on the phase-transition behavior of free PNIPAM molecules and hydrogels in bulk solution have been intensively investigated,[28−33] there have been very few studies of the salt effect for grafted PNIPAM on solid surfaces. Kizhakkedathu et al.[34] have synthesized a polystyrene latex sample with surface grafted PNIPAM and found that the hydrodynamic thickness of the brush is sensitive to the concentration of sodium chloride and sodium sulfate solutions. Jhon et al.[35] used QCM to determine the phase-transition temperature of the grafted PNIPAM in sodium chloride solution by attaching the polymer directly onto a QCM sensor. Interestingly, they pointed out that reduction in phase-transition temperature by the addition of sodium chloride is similar to that seen for free PNIPAM in solution. To date, however, these studies have focused mainly on the vertical dimensions of the collapsing layer, and no direct morphological information has been obtained. In addition, information concerning the kinetics of the structural change for grafted PNIPAM has also not been fully reported to date.

Recently, we reported the in situ observation of a relatively low-graft density PNIPAM layer of high molecular weight using an atomic force microscope (AFM).[36] In this work, we successfully visualized the PNIPAM layer structural changes as a

* To whom correspondence should be addressed. E-mail: s.r.biggs@leeds.ac.uk.
† University of Leeds.
‡ National Institute of Advanced Industrial Science and Technology.

10.1021/ma071878e CCC: $37.00
Published on Web 11/10/2007

function of temperature across the LCST. In addition, we also used a quartz crystal microbalance (QCM) to obtain related quantitative information about these conformational changes under the same conditions. Under the conditions of the experiments reported, the polymer layer showed a sharp transition at the LCST, which corresponded to that expected in the bulk, from an expanded brush to a collapsed mushroom-like layer. In addition, the AFM and QCM-D data suggested that further increases in temperature above the LCST resulted in further dehydration of the collapsed layer and the formation of smaller, tighter, polymer coils.

The QCM is a very sensitive tool for the determination of mass on flat substrates. Recently, it has become a popular tool for examining adsorption at the solid−liquid interface with an additional technique using the dissipation signal available from the resonance decay.[37,38] In the case of the grafted polymer, we have conducted QCM experiments in a previous paper using a sensor onto which a PNIPAM layer was directly attached. We found that the QCM-D data showed a significant change at the LCST corresponding to the structural behavior of the PNIPAM. Also, further structural changes above and below the LCST were apparent that were not easily seen in the AFM images of the same system. This suggests that QCM-D may be used as a powerful tool for the investigation of complex structural changes in the polymer films at the solid−liquid interface.

In our previous work, we only explored water without any salts as the background solution. Here, we report the results of an investigation into salt-induced morphological behavior for grafted PNIPAM films at a constant temperature. Our aim is to explore whether there are any significant differences in the nature of the transition when driven either by temperature or by salt. The experiments were conducted in sodium sulfate solutions across a wide range of concentration. We chose sodium sulfate as the salt because of its very strong salting-out effect, mentioned above. The surfaces used here were the same ones as reported in our previous paper that exhibited a sharp and significant structural change from brush-like to mushroom-like at the LCST. As before, we investigated this system using a combination of in situ AFM imaging, AFM force−distance data, and QCM-D measurements.

Experimental Section

Materials. Silicon wafers (Nilaco, Japan) were used as test surfaces, and they were cut in ca. 1.5 × 1.5 cm pieces. Polished, AT-cut quartz crystal QCM sensors (1.4 cm in diameter) with a coating of a thin silicon oxide layer obtained from Q-Sense AB (Sweden) were used for QCM measurements. *N*-Isopropylacrylamide (NIPAAm) was obtained from Aldrich and recrystallized from hexane. Potassium persulfate and *N*,*N*,*N*′,*N*′-tetramethylethylenediamine (TMEDA) of synthesis grade were obtained from Aldrich and used without further purification. Dimethylvinylchlorosilane, toluene, chloroform, and sodium sulfate of reagent grade (Aldrich) were used as received. All water used in experiments was purified using a Milli-Q system (Millipore).

Grafting of PNIPAM on Surfaces. The detailed method to prepare an end-grafted PNIPAM layer on both the silicon wafer surface and the QCM-D sensor has been given elsewhere.[36] Briefly, the silicon substrates were cleaned in a 7:3 mixture of concentrated sulfuric acid and hydrogen peroxide (piranha solution), while the QCM-D sensors were cleaned by UV irradiation prior to grafting. Next, they were immersed in a 1 mM dimethylvinylchlorosilane solution in toluene for 1 h to immobilize active vinyl moieties on the surface. After being washed with toluene and chloroform, and dried in a stream of nitrogen gas, the surfaces were immersed in a 15 wt % aqueous NIPAM solution in a Teflon reaction vessel, which was degassed by bubbling with nitrogen gas. Next, 0.2 mL of TMEDA and 0.01 g of potassium persulfate were added to initiate free radical graft polymerization, which proceeded at 4 °C for 12 h. After the reaction, the surface was washed with copious amounts of water and dried. The molecular weight of grafted PNIPAM was estimated by gel permeation chromatography (GPC, Waters) of free polymer generated in the bulk solution during the polymerization, which was collected by precipitation into cold methanol. A weight average molecular weight of the PNIPAM on the silicon wafer and the molecular weight on the QCM sensor was 655 and 715 kDa, respectively, using DMF with 0.01 M LiBr as mobile phase and polystyrene for calibration standards. The graft density of the PNIPAM on the silicon was 0.0088 chains/nm^2, calculated from dry thickness, 7.6 nm, measured with an ellipsometer (Gaertner Scientific) and molecular weight data assuming the dry density value of PNIPAM[40] to be 1.269 g/cm^3. The grafting density on the QCM sensor was 0.0074 chains/nm^2 calculated from the mass of grafted layer measured directly by the frequency of the sensor.

AFM Imaging. Images of the grafted polymer layers on silica in salt solution were captured using a Nanoscope IV atomic force microscope (Veeco Instruments). All images presented are height images collected using the soft-contact method[39] and have been zero-order flattened using a standard algorithm within the Nanoscope software. Microfabricated cantilevers with an integral silicon nitride tip (NanoProbe, Olympus) were used for all AFM experiments and were cleaned using UV irradiation prior to use. The solutions were passed through a 0.2 μm filter (GHP Acrodisc, Pall Gelman Science) mounted on a syringe when they were injected into the AFM fluid cell. The solution temperature was monitored with a small thermocouple inserted into the liquid cell, and experiments were conducted at 26.0 ± 0.2 °C. Prior to the imaging in every solution, water was injected first in the cell, and then it was exchanged to the salt solution of the given concentration after an interval of at least 15 min. The imaging usually started after the equilibration of the solution temperature for at least 30 min to ensure stability of the imaging.

QCM-D Measurements. The shifts in frequency (Δf) and dissipation (ΔD) for the sensor crystals at the third overtone (~15 MHz) were monitored using a commercial QCM-D (Q-300, Q-Sense AB). The temperature of the solution in the chamber was maintained at 26.0 °C with deviation of ±0.02 °C. As in the case of AFM imaging, water was injected first in the cell prior to the measurements at every concentration, then it was exchanged to the salt solution of the given concentration. For every solution, the values of Δf and ΔD were allowed to equilibrate for at least 30 min.

Results and Discussion

AFM Images. In situ soft contact AFM images of the PNIPAM layer obtained in various concentrations of Na_2SO_4 solutions at 26.0 °C are shown in Figure 1. In 0 M solution (water), the image was essentially flat, and only very subtle indications of any structural features can be seen. These features are likely related to the underlying roughness of the silica substrate and/or an unevenness of the polymer chain length due to the inherent polydispersity and are not indicative of any phase changes in the grafted polymer layer. After the salt concentration was increased to 0.1 M, the resultant image appears to give some weak indication of the presence of surface features. A further concentration increase to 0.12 M results in a large number of domain-like structures on the substrate now becoming clearly visible. At concentrations larger than 0.12 M, these structures were seen to remain and were easily recorded using the AFM. Interestingly, the size of the domains appears to become smaller, while the number of the domains increases with further increases in salt concentration. In addition, these structures generally became easier to image sharply as the salt concentration was increased.

Qualitatively, these results are quite similar to those reported previously by us for this system in water when the temperature

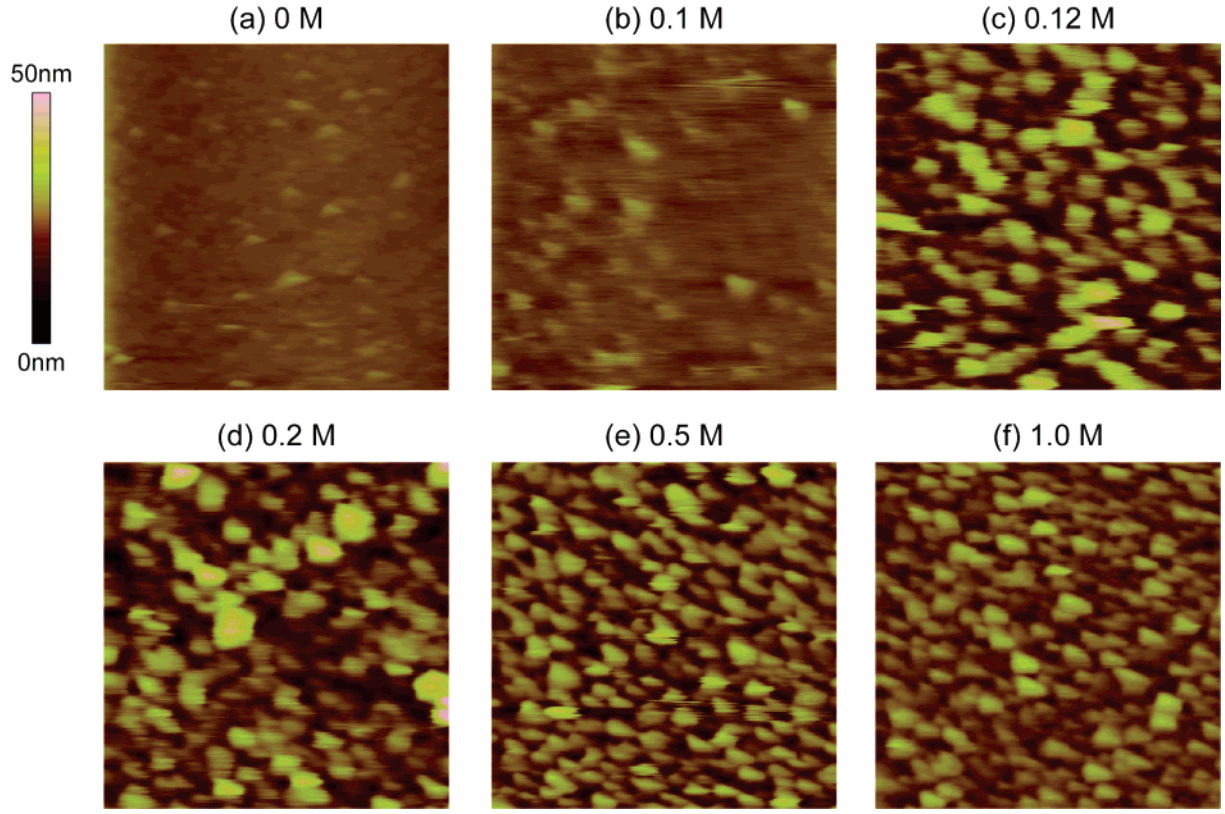

Figure 1. AFM images ($2 \times 2\ \mu m^2$) of a PNIPAM layer on silicon wafer in Na_2SO_4 solutions. Images were obtained in (a) 0, (b) 0.1, (c) 0.12, (d) 0.2, (e) 0.5, and (f) 1.0 M solutions. All images were obtained after an equilibration of at least 30 min.

was altered; in this case, similar domain structures were also seen to appear suddenly on the image at the LCST.[36] According to previous reports for the phase transition of free PNIPAM molecules and hydrogels,[28−33] the concentration of sulfate at which the phase transition occurs at 26 °C is in the range between 0.1 and 0.2 M. Our result from the AFM images (above) of a significant change at 0.1−0.12 M is therefore in good agreement with these earlier reports. Hence, we may conclude here that the AFM images are able to clearly visualize the phase transition for grafted PNIPAM chains from a "brush-like" to "mushroom-like" state, and this phase-transition concentration occurs between 0.1 and 0.12 M for the present system. The apparent diameter of the domains observed in the image is seen to be approximately 100−200 nm. Even taking into account some tip convolution effects on the images, these domain sizes imply that each collapsed structure contains a number of chains rather than being representative of single chains on the surface.

The phase transition of the grafted PNIPAM chains in our system occurs across a very narrow concentration range of between 0.1 and 0.12 M. Given this relatively narrow range, more detailed analysis of the transition using direct imaging was therefore undertaken in an attempt to see how exact the transition point was. We therefore took time-dependent AFM images in 0.10, 0.11, and 0.12 M solutions, starting from the moment immediately after the injection of the solution was completed. Data for the 0.11 M system are given in Figure 2. Initially, under these conditions, no specific features were seen in the image, and the surface morphology was very similar to that obtained in 0.10 M solution. Comparison of the image after 3 min, Figure 2a, with that at 0.10 M, Figure 1b, shows very little difference. However, after longer time periods at 0.11 M, some sharper features were seen to gradually appear, Figure 2b and c, and finally the domain-like structures were clearly seen on the image at 35 min as shown in Figure 2d. After this image, further significant change was not observed on the surface under these conditions. This rather slow process implies that the grafted PNIPAM is in a somewhat unstable state in this solution and that this concentration of sulfate ions must be extremely close to the transition point. Interestingly, the images at the other two concentrations reach equilibrium much faster than this despite the small difference of the concentration. At 0.10 M, the image showed very weakly structured features, which were very similar to those shown in Figure 1b, immediately after the injection of the solution (3 min). The image then showed little further change, indicating that equilibrium was rapidly attained. At 0.12 M, the change was slower than at 0.10 M but still much faster than at 0.11 M. The domain features were seen on the image immediately after the injection, and they then became steadily clearer over time. The image seen was essentially the same as Figure 1c after about 15 min, and there were no significant changes after that time.

In contrast, PNIPAM exhibits a very quick response to concentration when the system undergoes collapse in high concentration salt solutions, as shown in Figure 3. Here, the AFM image was first taken in water, then in 1.0 M solution starting immediately after the solution was injected of into the fluid cell, and finally in water again starting immediately after the Na_2SO_4 solution was replaced by water. After only 3 min since the injection of the 1.0 M Na_2SO_4 solution, which is practically the shortest period necessary to take one image in the present condition, the domain structures can already be clearly seen on the image. These features were completely stable, and no further changes in the surface morphology were seen after this point. Interestingly, after then rinsing this surface with water, there were no evident traces of any collapsed surface features remaining after 3 min from the injection of the water. These results indicate that, in the present system, the transition of the grafted PNIPAM chains from a brush-like to a mushroom-

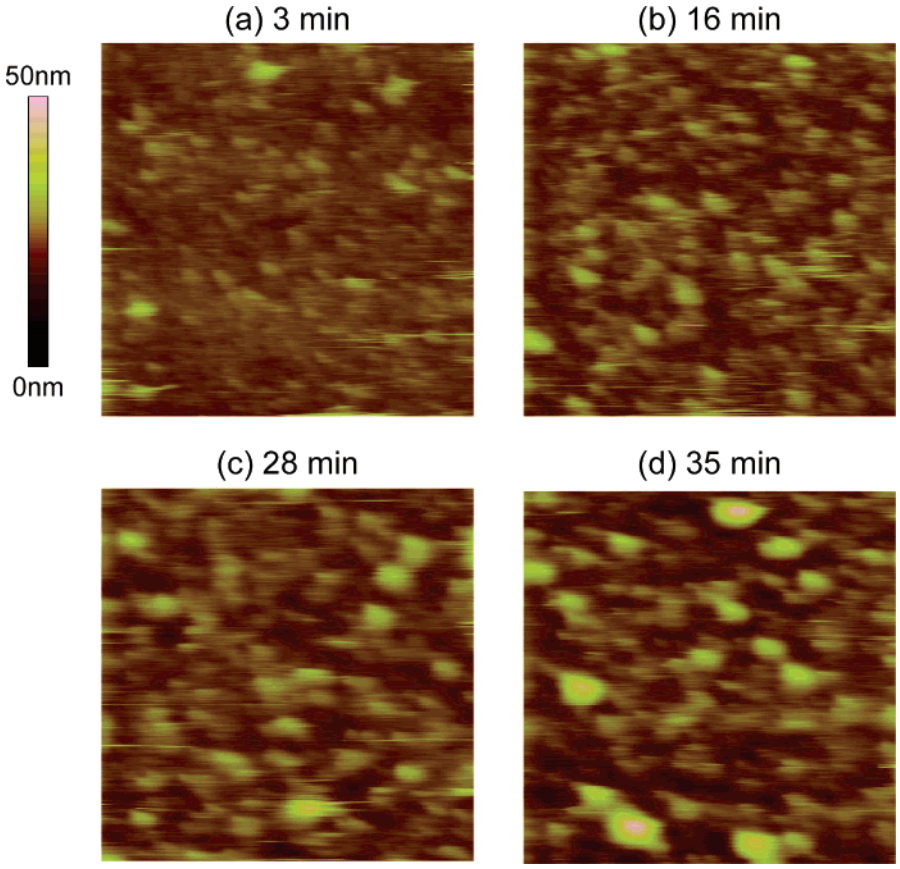

Figure 2. AFM images ($2 \times 2\ \mu m^2$) of a PNIPAM layer on silicon wafer in 0.11 M Na_2SO_4 solution. Image was taken at (a) 3, (b) 16, (c) 28, and (d) 35 min after the injection of the solution into AFM fluid cell.

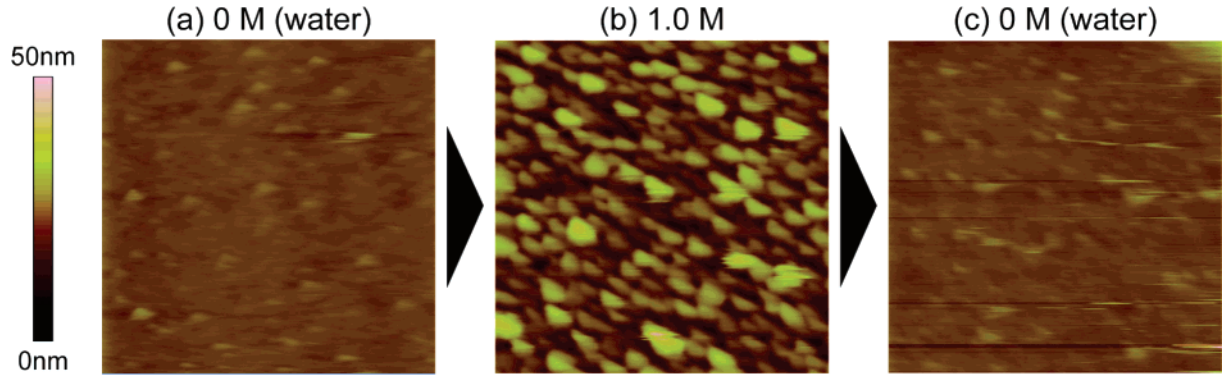

Figure 3. AFM images ($2 \times 2\ \mu m^2$) of a PNIPAM layer on silicon upon the change of the solution. Image was taken (a) in water, (b) in 1.0 M Na_2SO_4 solution at 3 min after the injection of the solution replacing water, and (c) in water at 3 min after the injection of water replacing 1.0 M Na_2SO_4 solution.

like state is fast and almost completely reversible, if the salt concentration is sufficiently high.

Interaction Forces between Probe Tip and Surface. In addition to the AFM imaging, interaction forces were also measured between the cantilever tip and the polymer layer at every concentration. The apparent separation distance between the surfaces was determined by simply assuming the constant compliance region of the raw force data (force versus piezo-position curve) to be zero distance.[41] It should be noted, however, that zero distances determined by this method are not true zero distances but indicate only the point of hard-wall contact where the grafted polymer layer no longer compresses under the cantilever tip. In reality, an offset is expected from the zero distance when there is a polymer layer on one or both surfaces. Therefore, in the present case, the separation distances given should be considered as a relative distance from an ill-defined zero position, the point of hard-wall contact. Notwithstanding this issue, it is possible to observe relative changes between force−distance curves depending on the solution concentration.

Typical force−distance curves when the cantilever tip approaches the grafted polymer substrate are given in Figure 4. At low concentration, a repulsive force was seen to commence at a large apparent separation distance in the force curves, and the extent of this repulsion is much greater than would be expected for any electrical double layer interactions. For instance, the expected Debye length of double-layer force in a 0.1 M divalent electrolyte solution is about 0.56 nm,[42] whereas the decay length of the repulsive force obtained at 0.1 M is more than 10 nm. Thus, we can attribute this repulsion to the steric repulsion of the grafted polymer brush resisting compression by the tip, and not an electrostatic repulsion. With

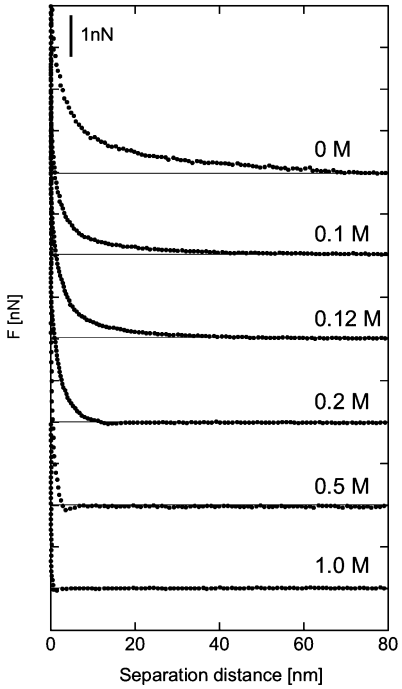

Figure 4. Force curves measured between the PNIPAM layer on silicon wafer and probe tip in Na_2SO_4 solutions at 0, 0.1, 0.12, 0.2, 0.5, and 1.0 M. The zero position of the tip is expediently defined as the starting position of the linear part in raw force data.

increasing concentration, the range of the repulsive force was seen to gradually decrease. It should be noted that no significant change in the shape of the force curve was observed at around 0.12 M, whereas the AFM image changes drastically at this concentration due to the phase transition. After the phase transition, the range of monotonically increasing repulsive interaction continues to decrease with increasing concentration, and finally the repulsive force is not observed in the force curves at high concentration. As seen in the figure, the force curves at 0.5 and 1.0 M consisted of a small attractive force and a very short-range steric force. This indicates the polymer aggregates on the surface are very stiff each and hardly deform in high concentration solution.

We also estimated change in the apparent thickness of the grafted layer as a function of concentration from the force−distance data. As mentioned above, there is considerable uncertainty in the position of zero-distance for the force data shown here. However, we might reasonably expect that the grafted layer thickness is identical to and independent of the salt concentration, when it is fully compressed under the tip.[22] If so, we can assume the range of the obtained repulsive forces to be representative of the relative thickness of the layer under different solution conditions. As shown in Figure 5, there is a strong dependence of the apparent layer thickness on the salt concentration. Even at low salt concentrations, a small increase of concentration causes a significant reduction in the apparent thickness of the repulsive steric layer. The change of the apparent layer thickness was seen to be steepest at the concentrations between 0.1 and 0.13 M corresponding directly with the expected position of the phase transition from the images. After phase transition, at concentrations larger than 0.13 M, the decrease in the thickness again became less steep but was still significant. This decreasing thickness after the phase transition is consistent with the observations from the AFM images that the domain structures become smaller and more compact at these higher concentrations.

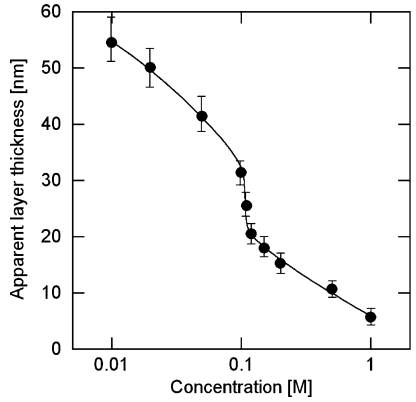

Figure 5. Change in the relative layer thickness as a function of concentration deduced from Figure 3. The error bars indicate the variation in data obtained at 10 different locations on the surface.

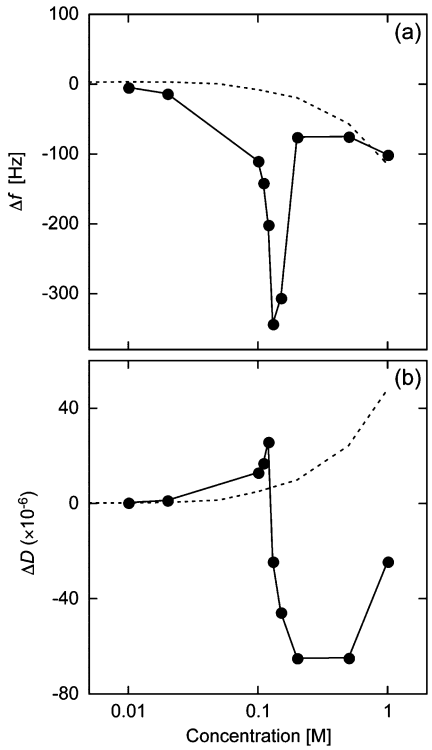

Figure 6. The changes in frequency, Δf (a), and dissipation, ΔD (b), as a function of Na_2SO_4 concentration for PNIPAM-coated crystal in water. The data for the bare crystal are shown as the dashed line.

QCM-D. Changes in Δf and ΔD as a function of salt concentration for a bare (uncoated) crystal and a PNIPAM-coated crystal are shown in Figure 6. Each data point in the graph indicates the equilibrium value at the given concentration. For the bare crystal, Δf decreases and ΔD increases with increasing salt concentration, shown as dotted lines in Figure 6. These changes can be attributed simply to the variation of the bulk viscosity and density when the salt concentration is altered as expected from standard QCM theory.

The behaviors of Δf and ΔD are dramatically altered when the crystal is coated with a PNIPAM layer. Below the expected transition point for the layer, predicted from the AFM images, the magnitude of Δf was seen to increase with increasing salt concentration more rapidly than for the bare crystal. This change was seen to become steeper with increasing concentration toward a salt concentration of 0.12 M, after which point the signal response showed a clear discontinuity. After this point, the magnitude of Δf was seen to decrease steeply over a narrow

concentration range before once again appearing to track the bare crystal data. The data for ΔD appear to increase along a pathway similar to that for the bare crystal at low salt concentrations, before showing some deviations from the bare crystal data at around 0.1 M. Above this point, ΔD increases steeply and reaches a maximum at 0.12 M before decreasing abruptly to reach a minimum value at 0.2 M. After this point, ΔD was seen to once again increase. It is important to note that the concentration around 0.12 M, at which the pronounced changes of Δf and ΔD happen, is correspondent to the phase-transition concentration estimated from the AFM images.

The observed changes in Δf are quite similar to those previously reported for the effects of temperature change in water in our previous paper:[36] Δf shows a large peak at the point at which the phase transition occurs. Therefore, we can suppose a similar interpretation for the Δf data here. Following the "traditional" interpretation of QCM-D data, larger negative values are interpreted as an increase in the adsorbed mass on the crystal surface as well as decreased viscosity and/or density of the surrounding solvent, if it is non-adsorbing. If the adsorbed mass of polymer is constant, as in the case for a grafted system such as that used here, changes in frequency, over and above those caused by the solvent conditions, must be caused by changes in the amount of liquid bound into the layer as a result of swelling or collapse. Thus, the significant apparent increase of mass coupled to the surface as the salt concentration increases toward the transition point (0.12 M) is unexpected because the coupled mass of liquid in the film should decrease as a result of the layer collapse.

To explain this discrepancy, we must take into account the structural changes of the grafted layer as the concentration is altered and the quality of the coupling between this layer and the oscillating crystal surface. Comparing Figures 5 and 6, one can observe that the apparent thickness of PNIPAM chains and the transition point for the system correspond well with changes in Δf. The initial decline in the value of Δf at low concentration corresponds to the gradual collapse of the layer with increasing concentration even well below the phase-transition point. The steeper decline of Δf toward the phase transition, between 0.1 and 0.13 M, is in good correspondence with the change in relative layer thickness.

The interpretation of QCM data is highly problematic because the system effectively senses the quality of the coupling between the oscillating crystal and the surrounding medium. As a result, direct conversion of the observed frequency shifts into an adsorbed mass should be treated with great caution, especially for swollen polymer films in solution such as those investigated here. Nonetheless, the data can in principle provide significant insights about structural changes in a layer, particularly when the mass of adsorbate is known from other sources and/or is fixed. Clearly, the data reported here appear counter-intuitive when considered against the standard analysis protocols using the Sauerbrey theory, as recommended by the manufacturer. In the brush-like state, the flexible and diffuse nature of the layer, especially at larger distances from the surface, may be expected to couple poorly with the oscillatory movement of the sensor crystal. In addition, the surrounding fluid can also move into and out of this outer part of the layer easily and so would not be detected. This latter point is important because the detected signal in QCM measurements is known to result from both the adsorbed polymer but also any "trapped" solvent in the film that moves in unison with the crystal. Obviously, the lateral shear of the crystal will establish a shear plane at some distance away from the surface and it is the mass inside this plane that is detected; clearly, the more diffuse is the polymer layer, the more we might expect a discrepancy between the true extent of the polymer layer and that detected using QCM for solvent and polymer moving with the crystal.

Upon dehydration and collapse, the grafted polymer chains must be able to more effectively couple with the motion of the oscillating sensor and more of the energy is effectively transferred. As a result, despite the fact that the mass of polymer is invariant and we might expect the true mass of solvent in the layer to decrease, we see a large change in the magnitude of Δf toward the phase-transition point. Such a change is commensurate with an increase in the rigidity of the adsorbed polymer chains, as expected when they begin to collapse. The surrounding fluid is then also expected to couple more efficiently with the motion of the layer and contribute to the observed signal. These effects result in the observed additional "effective mass" loaded on the surface.

The structure-change effect clearly exceeds any mass reduction caused by the water release from the surface due to dehydration below the phase-transition point. After the phase transition, however, the conformation change becomes less significant as shown in Figures 1 and 5. The large decrease in the magnitude of Δf after the phase transition must be related therefore to a significant and catastrophic dehydration of water from the chains, as expected at phase transition, and this effect becomes dominant resulting in the apparent "mass loss" seen here.

The changes seen in the dissipation data are broadly consistent with those discussed above. Close to, but below, the transition point the dissipation is seen to increase. Larger values of dissipation are generally interpreted as corresponding to an increased capacity to dissipate energy and hence a "softer" adsorbed layer. Clearly, this is not wholly consistent with the expected changes to the layer in this region and most probably is associated with the complex changes in the coupling of the layer discussed above. As a result, this region is not simple to interpret in terms of a real physical change. However, the sharp drop of ΔD around the phase-transition concentration clearly suggests strongly a large change to a more rigid layer consistent with the formation of a dense compact state for the polymer chains. Because a rigid layer will dissipate less energy than a flexible one,[43] ΔD shifts negatively. ΔD continues to decrease even after phase transition, up to 0.5 M. This result is in good agreement with the force curve data where the range of the repulsive force decreased significantly after the phase transition. Therefore, the shift in data would reflect the behavior that the PNIPAM chains continue to collapse even after phase transition, making increasingly rigid surface structures. This is also broadly consistent with the AFM images in Figure 1.

Figure 7 shows data for the changes in magnitude of Δf and ΔD after injecting 0.1, 0.11, and 1.0 M Na_2SO_4 solutions, as a function of time. In 0.1 and 1.0 M solutions, both signals show rapid equilibration immediately after injection and quickly reach a plateau value, within 3−4 min. In contrast, in 0.11 M solution, $-\Delta f$ exhibits a slow monotonic increase after the initial sharp increase, and it takes around 30 min for the signals to reach equilibrium. Note that, interestingly, the equilibration of ΔD is faster than that of Δf and occurs after about 10 min. These results correspond directly with the time-dependent AFM images shown in Figures 2 and 3, in which the images continued to change evidently with time at 0.11 M, whereas the domain structures were imaged sharply immediately after the injection of the solution, at 1.0 M. Interestingly, the time necessary for Δf to reach the equilibrium at 0.11 M is very close to the time

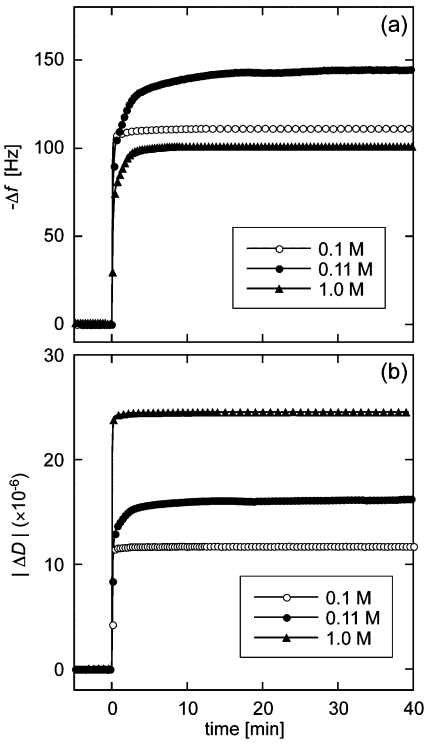

Figure 7. Changes in the values of $-\Delta f$ (a) and $|\Delta D|$ (b) obtained in 0.1, 0.11, and 1.0 M Na_2SO_4 solutions as a function of time.

after which AFM images show no change. Therefore, these data suggest that QCM can also detect dynamic structural changes of grafted polymer layers.

General Comments. From the AFM images obtained, it is clear that the phase transition of grafted PNIPAM from a "brush-like" to a "mushroom-like" state occurs over a narrow concentration range of added salt. The behavior of the grafted PNIPAM when the salt concentration is increased at fixed temperature is quite similar to that when the solution temperature is increased: The phase transition takes place sharply at a critical point of the concentration, about 0.12 M, and the PNIPAM chains change their structure significantly across a narrow concentration range.

From the images and force curve data, it is also suggested that, in the transition process, a vertical collapse of the chains seems to first take place and then strong aggregation of the chain follows. Even at concentration well below the phase-transition concentration, the grafted chains are seen to gradually collapse indicated as the decrease of the apparent layer thickness. At the phase-transition concentration, the chains suddenly aggregate laterally to form the collapsed "mushroom-like" structures, which appear on the AFM images. It has been reported that the strong salting-out anions like sulfate ion destabilize the hydrogen bonding between water molecules and the amide groups via polarization, even when they are added by small amounts.[32,33,44] By this destabilization, intra- and/or intermolecular hydrogen bonds will be formed between the segments of the PNIPAM chains. This results in the vertical collapse of the layer at the low concentration that proceeds gradually with increasing concentration. On the other hand, strong aggregation around the phase transition is likely to be driven by the attractive intra- and/or interchain interaction, a hydrophobic interaction. The hydrophobic interaction is suggested to act by the destruction of hydrophobic hydration of the hydrocarbons in the PNIPAM chains by the salt and to be enhanced by the reduction of the distance between the chains by the amide dehydration.[32]

Time dependence of the AFM images and the QCM data may give a basic picture for salt-induced kinetics of the structural behavior of the grafted PNIPAM on a solid surface. The very quick response of the PNIPAM layer to low or high concentration solutions is expected considering the sensitive nature of PNIPAM to the environmental conditions.[44] The reproducibility of the PNIPAM structures against the large change of concentration (Figure 3) can be related to the low grafting density of the surfaces used, which allows the individual chains to behave more freely. In contrast, the AFM images and QCM data confirmed a slow relaxation of the PNIPAM at 0.11 M, close to the phase-transition concentration. This change of the kinetics between narrow concentration range, 0.1 and 0.11 M, is surprising and might be a good example of a very delicate balance that lies between hydration of the chains and hydrophobic interaction. At 0.11 M, it is suggested that the dehydration is insufficient to induce the hydrophobic interaction among PNIPAM chains. Thus, aggregation of the chains is presumed to be dominated by the frequency of contacts between dehydrated hydrophobic groups within individual chains.[45] This may then drive a slow and gradual aggregation of the chains.

The changes in Δf and ΔD observed in the present study show an evident difference from the results reported in previous research using high-density PNIPAM layers prepared by a "grafting-from" method. Jhon et al.[35] used a layer prepared by ATRP and found that both signals showed a gradual and almost monotonic change with increasing NaCl concentration in a range from 0 to 1 M. This difference may be directly attributed to differences in the grafting density. A low grafting density of the polymer chains allows individual chains to behave more freely, resulting in the sharp structure transition across phase boundary. Consequently, Δf and ΔD values recorded in the present study showed significant changes across the critical phase-transition point. Similarly, the molecular weight (chain length) is likely to have a critical effect on the QCM data. Zhang[19] used a PNIPAM layer, which has a much smaller molecular weight than the present study adsorbed from solution, and found that Δf decreased monotonically throughout a temperature range between 20 and 38 °C. In this case, it is reasonable to consider that the structural collapse effect might be too weak to detect easily and the mass loss caused by dehydration dominates, resulting in the decrease of Δf.

The most evident difference between the structural change of the PNIPAM layer in water at various temperature given in ref 36 and that in sodium sulfate solutions is seen after the phase transition. In water, the PNIPAM chains are apparently still capable of deforming even after collapse to a globular state above the LCST, up to temperatures as high as 40 °C. In the sodium sulfate solutions, by contrast, the layer seems to become considerably more rigid and non-deformable, as indicated in the force curves at 0.5 and 1.0 M, as the salt concentration increases above the phase-transition point. This difference is also reflected in the measured ΔD values from the QCM data. While ΔD drops sharply across a very narrow temperature range at the LCST and shows very little change below and above the LCST in water, ΔD continues to decrease even after phase transition in Na_2SO_4 solution, up to 0.5 M. This implies that the chains can attain an almost fully collapsed, non-deformable state to make very rigid structure even after the phase transition in the Na_2SO_4 solution. It has been reported that in the case of the free PNIPAM polymers in water solution, many amide groups in the PNIPAM chains remain hydrated and the chains contain water in their structure even in their fully collapsed state at high temperature after phase transition.[45,46] Thus, it is not

unreasonable to suppose that water molecules continue to be released with increasing concentration even after the phase transition in the Na_2SO_4 solutions, because addition of the "salting-out" ions might disrupt the amide−water hydrogen bonds more effectively than raising temperature.[32] If less and less water remained in the chains with increasing concentration, it should result in the non-deformable layer at the high salt concentration. The dehydration might be also accelerated by the osmotic pressure difference of the bulk solution and the layer.[47] This would be able to suck water trapped into the aggregates of the chains. These effects would make the mushroom structure rigid in the high concentration solutions.

Conclusion

In the present study, the salt-induced structural change of PNIPAM layer grafted on a flat surface was characterized in Na_2SO_4 solutions by AFM imaging. A considerable change in the shape of the brush-to-mushroom transition of PNIPAM chains was successfully visualized on the AFM images. The phase-transition behavior of grafted PNIPAM on a silica surface is also investigated using QCM. Both frequency and dissipation showed a sharp and significant change at around the phase-transition concentration, indicating that the phase transition of PNIPAM was detected clearly.

References and Notes

(1) Heskins, M.; Guillet, J. E. *J. Macromol. Sci. Chem.* **1968**, *A2*, 1441−1455.
(2) Kanazawa, H.; Yamamoto, K.; Matsushima, Y.; Kikuchi, A.; Sakurai, Y.; Okano, T. *Anal. Chem.* **1996**, *68*, 100−105.
(3) Kobayashi, J.; Kikuchi, A.; Sakai, K.; Okano, T. *Anal. Chem.* **2001**, *73*, 2027−2033.
(4) Osada, Y.; Honda, H.; Ohta, M. *J. Membr. Sci.* **1986**, *27*, 327−338.
(5) Park, Y. S.; Ito, Y.; Imanishi, Y. *Langmuir* **1998**, *14*, 910−914.
(6) Chen, J. H.; Yoshida, M.; Maekawa, Y.; Tsubokawa, N. *Polymer* **2001**, *42*, 9361−9365.
(7) Yoshioka, H.; Mikami, M.; Nakai, T.; Mori, Y. *Polym. Adv. Technol.* **1994**, *6*, 418−420.
(8) Okano, T.; Yamada, N.; Okuhara, M.; Sakai, H.; Sakurai, Y. *Biomaterials* **1995**, *16*, 297−303.
(9) Okano, T.; Kikuchi, A.; Sakurai, Y.; Takei, Y.; Ogata, N. *J. Controlled Release* **1995**, *36*, 125−133.
(10) Cunliffe, D.; Alarcon, C. D.; Peters, V.; Smith, J. R.; Alexander, C. *Langmuir* **2003**, *19*, 2888−2899.
(11) Ionov, L.; Stamm, M.; Diez, S. *Nano Lett.* **2006**, *9*, 1982−1987.
(12) Walldal, C.; Wall, S. *Colloid Polym. Sci.* **2000**, *278*, 936−945.
(13) Zhu, P. W.; Napper, D. H. *J. Chem. Phys.* **1997**, *106*, 6492−6498.
(14) Balamurugan, S.; Mendez, S.; Balamurugan, S. S.; O'Brien, M. J.; Lopez, G. P. *Langmuir* **2003**, *19*, 2545−2549.
(15) Yim, H.; Kent, M. S.; Mendez, S.; Balamurugan, S. S.; Balamurugan, S.; Lopez, G. P.; Satija, S. *Macromolecules* **2004**, *37*, 1994−1997.
(16) Yim, H.; Kent, M. S.; Satija, S.; Mendez, S.; Balamurugan, S. S.; Balamurugan, S.; Lopez, G. P. *Phys. Rev. E* **2005**, *72*, 051801.
(17) Yim, H.; Kent, M. S.; Mendez, S.; Lopez, G. P.; Satija, S.; Seo, Y. *Macromolecules* **2006**, *39*, 3420−3426.
(18) Yim, H.; Kent, M. S.; Satija, S.; Mendez, S.; Balamurugan, S. S.; Balamurugan S.; Lopez, C. P. *J. Polym. Sci., Part B: Polym. Phys.* **2004**, *42*, 3302−3310.
(19) Zhang, G. *Macromolecules* **2004**, *37*, 6553−6557.
(20) Liu, G.; Zhang, G. *J. Phys. Chem. B* **2005**, *109*, 743−747.
(21) Liu, G.; Cheng, H.; Yan, L.; Zhang, G. *J. Phys. Chem. B* **2005**, *109*, 22603−22607.
(22) Kidoaki, S.; Ohya, S.; Nakayama, Y.; Matsuda, T. *Langmuir* **2001**, *17*, 2402−2407.
(23) Ishida, N.; Kobayashi, K. *J. Colloid Interface Sci.* **2006**, *297*, 513−519.
(24) Karlstrom, G.; Carlsson, A.; Lindman, B. *J. Phys. Chem.* **1990**, *94*, 5005−5015.
(25) Kundu, P. P.; Kundu, M. *Polymer* **2001**, *42*, 2015−2020.
(26) Von Hippel, P. H.; Schleich, T. In *Structure and Stability of Biological Macromolecules*; Timasheff, S. N., Fasman, G. D., Eds.; Marcel Dekker: New York, 1969; Chapter 6, pp 417−574.
(27) Von Hippel, P. H.; Wong, K. Y. *Science* **1964**, *145*, 577−580.
(28) Schild, H. G.; Tirrell, D. A. *J. Phys. Chem.* **1990**, *94*, 4352−4356.
(29) Inomata, H.; Goto, S.; Otake, K.; Saito, S. *Langmuir* **1992**, *8*, 687−690.
(30) Park, T. G.; Hoffman, A. S. *Macromolecules* **1993**, *26*, 5045−5048.
(31) Freitag, R.; Garret-Flaudy, F. *Langmuir* **2002**, *18*, 3434−3440.
(32) Paz, Y.; Kesselman, E.; Fahoum, L.; Portnaya, I.; Ramon, O. *J. Polym. Sci., Part B: Polym. Phys.* **2004**, *42*, 33−46.
(33) Zhang, Y.; Furyk, S.; Bergbreiter, D. E.; Cremer, P. S. *J. Am. Chem. Soc.* **2005**, *127*, 14505−14510.
(34) Kizhakkedathu, J. N.; Norris-Jones, R.; Brooks, D. E. *Macromolecules* **2004**, *37*, 734−743
(35) Jhon, Y. K.; Bhat, R. R.; Jeong, C.; Rojas, O. J.; Szleifer, I.; Genzer, J. *Macromol. Rapid Commun.* **2006**, *27*, 697−701
(36) Ishida, N.; Biggs, S. *Langmuir*, in press.
(37) Rodahl, M.; Höök, F.; Krozer, A.; Brzezinski, P.; Kasemo, B. *Rev. Sci. Instrum.* **1995**, *66*, 3924−3930.
(38) Rodahl, M.; Kasemo, B. *Rev. Sci. Instrum.* **1996**, *67*, 3238−3241.
(39) Manne, S.; Cleveland, J. P.; Gaub, H. E.; Stucky, G. D.; Hansma, P. K. *Langmuir* **1994**, *10*, 4409−4413.
(40) Lele, A. K.; Hirve, M. M.; Badiger, M. V.; Mashelkar, R. A. *Macromolecules* **1997**, *30*, 157−159.
(41) Ducker, W. A.; Senden, T. J.; Pashley, R. M. *Langmuir* **1992**, *8*, 1831−1836.
(42) Israelachvili, J. N. *Intermolecular and Surface Forces*, 2nd ed.; Academic Press: San Diego, 1992; p 238.
(43) Höök, F.; Kasemo, B.; Nylander, T.; Fant, C.; Sott, K.; Elwing, H. *Anal. Chem.* **2001**, *73*, 5796−5804.
(44) Yuan, G.; Wang, X.; Han, C. C.; Wu, C. *Macromolecules* **2006**, *39*, 6207−6209.
(45) Wang, X.; Qiu, X.; Wu, C. *Macromolecules* **1998**, *31*, 2972−2976.
(46) Maeda, Y.; Higuchi, T.; Ikeda, I. *Langmuir* **2000**, *16*, 7503−7509.
(47) Livney, Y.; Ramon, O.; Kesselman, E.; Cogan, U.; Mizrahi, S.; Cohen, Y. *J. Polym. Sci., Part B: Polym. Phys.* **2001**, *39*, 2740−2750.

MA071878E